

# A Combined $QFT/H_\infty$ Design Technique for TDOF Uncertain Feedback Systems

**Marcel Sidi**

Center for Technological Education Holon  
affiliated with TEL-AVIV University  
e-mail: sidi(barley.cteh.ac.il); fax: 972-3-5365285

**Abstract:** The present paper presents a way to incorporate  $QFT$  principles to the  $H_\infty$  control design technique to solve the Two-Degree of Freedom Feedback Problem with Highly Uncertain Plants. The proposed design procedure is illustrated with SISO and MIMO design examples for highly uncertain plants.

## 1- Introduction

Both  $QFT$  and  $H_\infty$  design techniques occupies the control community for a long time, from the beginning of the 70's. The so called today  $QFT$  design technique was first introduced in Horowitz and Sidi (1972), while the  $H_\infty$  norm as conceived today was first introduced by Zames (1976), (1979), and Zames and Francis (1983) to formulate the problem of sensitivity reduction by feedback as an  $H_\infty$  optimization problem. In the following years, the oriented design techniques for robust feedback systems has enormously expanded and developed for solving the robust feedback problem, Doyle 1978, Doyle and Stein (1981), Francis and Doyle (1986), Francis (1986), Zhou and Doyle (1998) and many others. During the past twenty years it was felt that there exist a very pronounced schism between the two techniques having the same design task, namely, robust design for uncertain feedback systems. Fortunately it is felt today that there exist a lot of parallelism between both design philosophies which can complement each other. The aim of this paper is to show how both techniques can be applied in a combined and efficient way to design two degree of freedom (TDOF) uncertain feedback systems, SISO and MIMO.

## 2. Parallelism between the $QFT$ and the $H_\infty$ norm design techniques.

The  $QFT$  for SISO and MIMO feedback systems is defined and solved in the classical frequency domain using Nyquist, Bode and Nichols oriented design techniques. The  $H_\infty$  norm design technique uses basically the state-space formulation for solving the feedback problem optimization, although the process and the desired performances to be achieved are specified once more in the frequency domain. A short review of both techniques follow.

**A. The  $QFT$  design technique** (It is assumed that the reader is familiar with this technique, if not, it is recommended to have a look in Horowitz and Sidi (1972) for the SISO case).



\* *Disturbance rejection specifications:* There is given a function  $D(\omega)$  that specifies the output specifications on  $T_d(j\omega)$ , in the form: For all  $P \in \{P\}$

$$|T_d(j\omega)| \leq D(\omega) \quad (4)$$

where

$$T_d(s) = \frac{y_d(s)}{d(s)} = \frac{1}{1 + G(s)P(s)} \stackrel{def}{=} S(s) \quad (5)$$

\* *Peaking of the disturbance rejection transfer function gains.*

In order to avoid too underdamped closed-loop TFs, there are given limits in the form of two numbers,  $\beta$  and  $\gamma$ , such that

$$|T_1(j\omega)|_{\max} \leq \beta \quad (6)$$

and

$$|T_d(j\omega)|_{\max} \equiv |S(j\omega)|_{\max} \leq \gamma \quad (7)$$

where

$$T_1(s) = \frac{G(s)P(s)}{1 + G(s)P(s)} \quad (8)$$

$T_1(s)$  stands for the unity feedback closed-loop TF, with no prefilter  $F(s)$ . This is the one degree of freedom (ODOF) standard tracking input/output TF.

\* *Sensor noise amplification.* Another important TF is related to the amplification of the sensor noise  $n$ .

$$T_{un} = \frac{u(s)}{n(s)} = \frac{G(s)}{1 + G(s)P(s)} = G(s)S(s) \quad (9)$$

This TF is responsible for the level of control effort, which, if not carefully limited, may lead to control effort saturation with the immediate consequence of causing instability to the feedback system.

\* *Design of the inner compensator  $G(s)$ ;* 1st DOF. The nominal open-loop gain  $L_n(j\omega)$  is designed so that the obtained bounds on  $L_n(j\omega)$  in the Nichols chart are all satisfied for all plant cases, thus guaranteeing that overall gain changes  $\Delta|T(j\omega)|$  are smaller than those included between the upper and lower tracking specification bounds in Fig.2. A desired design criterion tends to minimize the amplification of the sensor noise  $n$  that spoils the control effort  $u$  in Fig.1. Sensor noise spectrum is usually at high frequencies, much higher than the active frequency range where sensitivity specifications and disturbances attenuation are considered. Hence, this is approximately achieved by asking for minimization of  $k$  defined in  $\lim_{s \rightarrow \infty} L_n(s) \rightarrow k/s^e$ , where  $e$  is the number of excess of poles over zeros at infinity. Moreover, the designed inner compensator  $G(s)$  is to be strictly proper.

\**Design of the prefilter  $F(s)$ : 2nd DOF.* With the obtained  $G(s)$  in the previous step, the unity feedback closed-loop TF  $|T_1(j\omega)|$  gains of all plant cases are plotted on Bode plots, as in Fig.2. Their maximum changes at all frequencies are equal or smaller than the permitted changes defined by the permitted bounds in the same figure. However, most probably, they all lie outside these bounds. The prefilter  $F(s)$  is designed in this step, whose task is to move all  $|T_1(j\omega)|$ s inside the permitted upper and lower bounds through the identity  $|T(j\omega)| = |T_1(j\omega)||F(j\omega)|$ .

\* Finally, the designed controller  $G(s)$  and prefilter  $F(s)$  guarantee that for all plants  $P \in \{P\}$  and/or all disturbances  $d \in \{d\}$  introduced in  $d$ , Fig.1, the system is stable and Eqs.(2) , (4), (6) and (7) are satisfied while minimization of the sensor noise amplification at the input to the plant is attained.

This completes the short review of *QFT*.

### ***B. $H_\infty$ norm optimization in control design.***

It is well known that the sensitivity function  $S(j\omega)$  and the complementary function  $T_1(j\omega)$  play an important part in control design. Most design specifications can be defined in term of these functions, which are related between them as follows:  $S(j\omega) + T_1(j\omega) = 1$ . Hence, they cannot both be specified and realized independently.

In general, in order to fulfill some design specifications, for instance disturbance attenuation, Eq.(4), the sensitivity function will be constrained to satisfy some norm inequality, for instance, the  $H_\infty$  norm, in the following way:  $\|S(j\omega)\|_\infty < M$ . In general,  $M$  will be frequency dependent, so that , define

$$|S(j\omega)| < 1/|W_s(j\omega)| \quad (10)$$

which is equivalent to satisfying

$$\|W_s(j\omega)S(j\omega)\|_\infty < 1 \quad (11)$$

where  $W_s(j\omega)$  is a weighting function related to the sensitivity function  $S(j\omega)$ .

If  $|S(j\omega)|$  is the only specified function of interest to the feedback control problem, then a weighting function  $W_s(j\omega)$  is first to be found, then, design the compensator  $G(s)$  by any optimization algorithm so that Eq.(11) is satisfied for all frequencies. In practice, more than one function need to be specified and the specifications satisfied, for instance,

$$\|W_{un}(j\omega)T_{un}(j\omega)\|_\infty < 1 , \|W_1(j\omega)T_1(j\omega)\|_\infty < 1 , \|W_s(j\omega)S(j\omega)\|_\infty < 1 \quad (12)$$

This is definitely impossible if the " $<$ " sign is exchanged with the " $=$ " sign because in a two degree of freedom feedback system only two compensator networks , $G(s)$  and  $F(s)$ , can be used at will for design purposes. The engineer then has to compromise between

achievement of the different specifications. Tradeoff is a common practice without which no engineering design can be completed.

*Mixed sensitivity* is a way to obtain a design when more than two specifications are to be achieved in a TDOF feedback system, and more than one specification in a ODOF system. Let us suppose that the system is ODOF. Then, we can define the different specifications in a stacked vector form, a performance vector  $\mathbf{PV}$ , in which all the important specifications in term of weighting functions are mixed together, for instance

$$\mathbf{PV} = \begin{bmatrix} W_S(j\omega)S(j\omega) \\ W_1(j\omega)T_1(j\omega) \\ W_{un}(j\omega)T_{un}(j\omega) \end{bmatrix} = \begin{bmatrix} W_S(j\omega)S(j\omega) \\ W_1(j\omega)G(j\omega)P(j\omega)S(j\omega) \\ W_{un}(j\omega)G(j\omega)S(j\omega) \end{bmatrix}$$

We have in this case a *mixed sensitivity specification*, Verma and Jonckheere (1984), Skogestad and Postlethwaite (1996). In this and future discussions, all weighting functions are assumed to be stable and NMP. For SISO systems, an Euclidean vector norm can be used for the overall design specification

$$\|\mathbf{PV}(j\omega)\|_\infty = \max_{\omega} \sqrt{|W_S S|^2 + |W_1 T_1|^2 + |W_{un} T_{un}|^2} < 1 \quad (13)$$

With this definition, a norm problem to be solved is of the form

$$\min_{G(s)} \|\mathbf{PV}(G)\|_\infty \quad (14)$$

where  $G(s)$  is the stabilizing compensator. In the MIMO case,  $\mathbf{PV}$  is a matrix, and principal gains (frequency dependent singular values) are used to measure the size of the optimized matrix. Solution of Eq.(12) is not exactly the solution of Eq.(13) which is attractive from mathematical point of view, and is also more conservative. This is especially pronounced when the peaking of the three involved functions have their maximum approximately at the same frequency. If  $n$  specified requirements are involved in Eq.(12), then solution per Eq.(13) may cause to an error in the achieved specifications by at most a factor of  $\sqrt{n}$ .

Remember that the three TFs  $S(s)$ ,  $T_1(s)$  and  $T_{un}(s)$  include the plant  $P(s)$ , which is meanwhile considerate to be known and fixed (no uncertainties). The compensator  $G(s)$  is an output of a solution of the optimization process in Eq.(14) performed by any existing algorithm such as the *hinfsyn* of  $\mu$ -Analysis and Synthesis TOOLBOX or the *hinf* of Robust Control TOOLBOX, or *hinfmi* of the LMI Control Toolbox, all of them belonging to The MATH WORKS Inc. In this context, the uncertainty of the plant is to be defined. There exist several modeling structures, one of the most popular of them being the multiplicative perturbation modeling, shown in Fig.3, in which

$$P(s) = P_n(s)[1 + W_{MP}(s)\Delta_{MP}(s)]; \quad \Delta_{MP}(j\omega) \leq 1 \quad \forall \omega \quad (15)$$

The subscript  $MP$  stands for *Multiplicative Perturbation*.

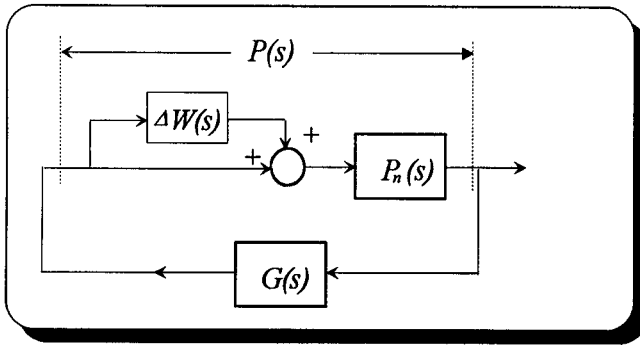


**Figure 3.** Multiplicative perturbation modeling of the plant.

This structure is very general and, as such, allows modeling of many different kinds of plant uncertainties. We can use Eq.(15) to model the uncertain plant in the following way: rewrite it as

$$\frac{P(j\omega) - P_n(j\omega)}{P_n(j\omega)} = W_{MP}(j\omega)\Delta_{MP}(j\omega); \quad |\Delta_{MP}(j\omega)| \leq 1 \quad (16)$$

Calculate for each frequency the maximum value of the left side of Eq.(16) for the entire uncertain set  $\{P(j\omega)\}$ . Call it  $\delta_{MP}(\omega)$ , namely:

$$\delta_{MP}(\omega) = \max_{\{P(j\omega)\}} \left| \frac{P(j\omega) - P_n(j\omega)}{P_n(j\omega)} \right| \quad (17)$$

By Eq.(16), the weighting function  $W_{MP}(j\omega)$  must satisfy

$$|W_{MP}(j\omega)| \geq \delta_{MP}(\omega)_{\max}, \quad \forall \omega \quad (18)$$

Very complicated and general uncertain plants can be modeled by use of Eqs.(17) and (18), which are next used to ascertain *robust stability*, which means, stability for all plants in the family  $\{P(s)\}$ . The condition for robust stability is summarized in the following theorem, see for instance Doyle et.al (1992).

**Theorem 1:** For *multiplicative modeled* uncertain plant  $P(s)$  the compensator  $G(s)$  provides robust stability iff

$$\|W_{MP}(s)T_1(s)\| < 1 \quad (19)$$

With this result, it is possible to redefine the sensitivity function  $W_{MP}(s) = W_1(s)$  in Eq.(13) so that stability is guaranteed for the entire set of plants in  $\{P(s)\}$ . (A similar theorem exist for MIMO feedback systems.)

*The basic problem in  $H_\infty$  control design is to define correctly the weighting functions so that the control design will come up with a solution that satisfies in the best way all design requirements.*

**Weighting function selection**

Weight selection of the different functions in Eq.(12) or (13) are the initial stage in a feedback system design using the  $H_\infty$  norm optimization. This is done on the basis of defined performance specifications by the customer. For instance, for known turbulence disturbances acting on an aircraft, an attenuation factor for disturbance can be defined in different frequencies, thus putting extremal limits on  $|S(j\omega)|$  such as its higher corner frequency; thus,  $W_s(s)$  can be explicitly defined. Moreover, in order to guarantee permitted steady state errors in following different external command inputs, additional constrains on  $|S(j\omega)|$  are defined and  $W_s(s)$  is accordingly manipulated to its final form. Selection of  $W_1(s)$  is based on desired input output properties on  $T_1(j\omega)$  which cannot be achieved independently of  $S(j\omega)$  because of the identity  $S(s)+T_1(s) = 1$ . The designer can find some reasonable way to define a compatible  $T_1(s)$  (hence also a compatible  $W_1(s)$ ), however, its final achieved form must also comply with  $W_{MP}(j\omega)$  (for the multiplicative modeling in our case) so that robust stability is guaranteed for all plant conditions.  $W_{un}(s)$  is generally generated according to acceptable control effort, due to sensor noise and to reference control inputs data for the control problem at hand. This is the situation when a ODOF control problem is to be solved. With the weighting functions so defined, the  $H_\infty$  control problem setup is as shown in Fig. (4) below, similar to that of Fig. 1 in which the weighting functions are incorporated.

The *mixed sensitivity problem* defined in Eqs.(13) and (14) is a special case of the so-called Standard  $H_\infty$  -Optimal Regulator Problem introduced by Doyle (1983), see also Kwakernaak (1993) and Skogestad and Postletwaite (1996). The structure in Fig.4b is that of the Standard  $H_\infty$  -Optimal Regulator derived from the feedback control setup of Fig.4a using the following relations:

$$\begin{aligned} z_1(s) &= -G(s)S(s)W_{un}(s)n(s) = T_{un}W_{un}n(s) \\ z_2(s) &= T_{uf}(s)W_{MP}(s)r_1(s) = T_{uf}W_{MP}r(s); [F(s) = 1] \\ z_3(s) &= S(s)W_s(s)d(s) \end{aligned} \tag{20}$$

$T_{uf}(s) \equiv T_1(s)$  in Eq.(8)

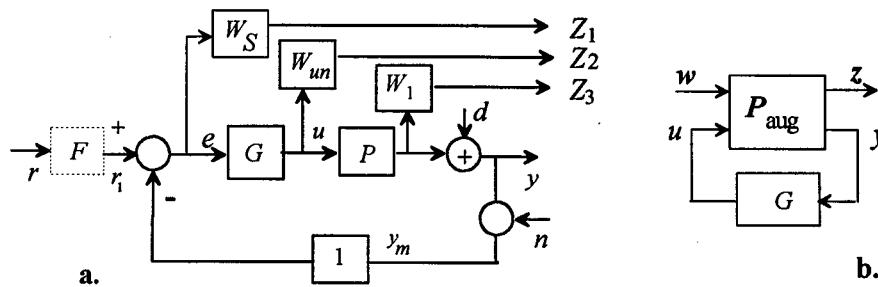


**Figure 4.** The mixed sensitivity standard problem with an added optional prefilter  $F(s)$  for solving the TDOF uncertain problem .

With the above adapted canonic structure we can define an input vector  $w(s) = \text{col}[d(s), n(s), r_1(s)]$  and an output vector  $z(s) = \text{col}[z_1(s), z_2(s), z_3(s)]$ . The signal vector  $z$  is in fact a system error vector to be minimized as per Eq.(14). In a ODOF feedback system Eq.(20) can be also derived by use of one sole input  $d$ ,  $n$  or  $r_1$ , let us decide on  $w=d$ . Moreover

$$\begin{aligned} z_1(s) &= W_{un}(s) u \\ z_2(s) &= W_{MP}(s) P(s)u \\ z_3(s) &= W_s(s)[w + P(s)u] \\ e &= -w - y = -w - P(s)u \end{aligned} \quad (21)$$

The above identified are used to obtain a generalized plant  $P_{\text{aug}}$  so that the structure in Fig.4a can be presented as in Fig.4b which has a more general interpretation than just the mixed sensitivity problem. The structure in Fig.4b applies for any MIMO control feedback system, but in the context of this explanation the SISO case is intended. The generalized plant  $P_{\text{aug}}$  in Fig.4b can be seen as an augmented plant in which  $w(s)$  is a vector of external inputs (such as  $r(s)$ ,  $d(s)$ ,  $n(s)$  in Fig.4a),  $u(s)$  is the controlling input to the SISO plant,  $z(s)$  is a vector of weighted external outputs (system errors such as PV in Eq.(13)), and  $e$  is the sensed error delivered to the compensator  $G(s)$ . In a MIMO feedback system, to be treated later,  $u$  and  $e$  become vectors too. The general control problem is then to find the compensator  $G(s)$  so that the norm of the closed-loop TF  $\|T_{wz}\|$  from  $w$  to  $z$  is minimized, minimize  $\|T_{wz}\|_{\infty}$ .

### c. Parallelism between the QFT and the $H_{\infty}$ norm design techniques.

Having discussed shortly both design techniques, it is of interest to point on existing parallelism between them, but also on existing shortcomings, so that potential complementation between the QFT and  $H_{\infty}$  design techniques may be performed in an useful way.

1-A gross difference between the shortly explained design techniques is the fact that with the  $H_{\infty}$  design technique, closed-loop tracking input/output permitted bounds on the time response are not specified for all plant conditions in the family  $\{P(s)\}$ . Hence, a TDOF feedback problem is not solved systematically. On the other hand, when a nominal plant desired response is specified, it can be achieved by correct specification of the weighting function  $W_1(s)$ , so that a specified TF  $T_1(s)$  is achieved.

2- Robust stability can be achieved with the  $H_{\infty}$  design technique by calculating the maximum gain changes of the plant at all frequencies, obtaining the limiting weighting function  $W_{MP}(s)$ , Eq.(18), and satisfying Eq.(19). This is in some sense equivalent to the plant templates in the QFT design technique which must satisfy the Nyquist stability criterion in the Nichols chart. The elements of the plant template in the QFT technique are complex numbers, while the templates in the multiplicative perturbation modeling are real gains.

3- Maximum peaking in  $|T_1(j\omega)|$  and  $|S(j\omega)|$ ,  $\beta$  and  $\gamma$  respectively in Eqs.(6) and (7), are guaranteed with the QFT technique by manipulating the plant templates in the Nichols chart so that they do not cross the standard closed-loop  $|T_1(j\omega)| = \beta$  and  $|S(j\omega)| = \gamma$  contours in the

Nichols and the inverted Nichols charts. The same effect is achieved with the  $H_\infty$  design technique by defining the weighting functions  $1/|W_1(j\omega)|$  and  $1/|W_s(j\omega)|$  to have maximum peaking of  $\beta$  and  $\gamma$  db respectively so that  $|T_1(j\omega)|$  and  $|S(j\omega)|$  will have maximum peaking of  $\beta$  and  $\gamma$  db respectively.

4- Minimization of sensor noise amplification is obtained in the  $H_\infty$  technique by specifying the  $W_{un}(s)$ , and real minimization is sometimes obtained by iterating with the different choice of this weighting function. With the  $QFT$  design technique, minimization of sensor noise amplification is achieved inherently when manipulating the nominal open-loop TF  $L_n(j\omega)$  in the Nichols chart by tending to minimize its gain at the higher frequency range, while meantime satisfying the frequency dependent tracking sensitivity bounds.

5- The  $QFT$  is in a way a synthesis design, in the sense that with specified plant uncertainties and sensitivity input/output specifications, the boundaries on  $L_n(j\omega)$  are uniquely derived in the Nichols chart, and, based on them, the control solution is also unique. The  $H_\infty$  design is proceeded by solving Eq.(13) which comes to be an  $H_2$  optimization problem, thus the three specifications in Eq.(12) are not achieved exactly, and some tradeoff between the different weighting functions is necessary until a satisfactory solution is obtained.

6- In summary, both  $H_\infty$  and  $QFT$  techniques solve the same problem with equivalent specifications, except for tracking input/output sensitivity specifications that can be solved by adequately using the second degree of freedom and adding the prefilter  $F(s)$ .

The task of the present work is to use the second degree of freedom,  $F(s)$ , in the  $H_\infty$  design technique in a similar way that this is done with the  $QFT$  design paradigm.

### 3. $H_\infty$ - norm optimization used in design of TDof uncertain feedback system structures.

The present section deals with the last, but most important specifications concerning the tracking input/output transfer function of a TDof feedback system. This was the basic problem treated in  $QFT$  for linear stable, minimum or nonminimum phase, unstable or sampled feedback systems for which quantitative specifications on  $|T(j\omega)|$ , Eq.(2), are defined and achieved. A design procedure for a TDof feedback system using  $H_\infty$  norm optimization will be next derived. The basic idea is explained with the SISO uncertain feedback problem, and is extended to the MIMO case in Section 4. The basic design philosophy includes two principal stages:

**Stage 1:** Achieve tracking input/output quantitative sensitivity specifications defined in the form of **maximal permitted changes** in  $|T_1(j\omega)|$  by using the  $H_\infty$  -norm optimization design for robust performance specifications.

**Stage 2:** Use the prefilter  $F(s)$  (the second degree of freedom) to move the unity feedback closed-loop TF gain obtained in Stage 1 inside the permitted tracking bounds, Eq.(2).

Stage 1 consists in designing for robust performance specifications, as explained in the last section, but with an adequately defined sensitivity weighting function  $W_s(s)$  which will satisfy the *permitted level of changes* in  $|T_1(j\omega)|$ . We shall see that when the norm optimization is performed for the TDOF problem, definition of  $W_s(s)$  alone is not sufficient, the control effort weighting function  $W_{un}(s)$  influence also the design procedure and is finally used for fine tuning. This design stage is next discussed.

We turn out to the initial definition of the sensitivity function  $S(s)$  which is, according to Bode (1945)

$$S_P^T = \frac{\partial T/T}{\partial P/P} = \frac{d \ln(T)}{d \ln(P)} = \frac{1}{1 + G(s)P(s)} = \frac{1}{1 + L(s)} \quad (22)$$

The meaning of this equation is, as pointed by Bode in his basic theorem: *The variation in the final gain characteristic in db, per db changes in the gain of P, is reduced by feedback in the ratio  $[1 + L(s)]$ :1.*

Unfortunately, the above equation is defined and is exact for infinitesimal changes only, but can as well be used for finite changes, Horowitz (1963). Eq.(22) can be used in its simplest form, namely,

$$|S(j\omega)| = |\Delta T(j\omega)|_{\max} \text{ dB} / |\Delta P(j\omega)|_{\max} \text{ dB} \quad (23)$$

in which  $|\Delta T(j\omega)|_{\max}$  are the maximal permitted changes in  $|T(j\omega)|$  dB as per Eq.(2) and Fig.2.  $|\Delta P(j\omega)|_{\max}$  are the maximal changes in gain of the uncertain plant also in dB.

Once the nominal sensitivity function  $|S_n(j\omega)|$  is obtained,  $W_s(s)$  can be calculated for use in the design stage. It does not really matter that the basic sensitivity equation is correct for very small plant changes, which is not our case, because anyway when the  $H_\infty$  optimization algorithm is executed the achieved nominal sensitivity gain  $|S(j\omega)|$  will not follow exactly the apriory defined  $1/|W_s(j\omega)|$  since such algorithms minimize an Euclidean norm and none of the elements of the mixed sensitivity vector, Eq.(13), can be satisfied individually with an equality sign such as  $|S_n(j\omega)W_s(j\omega)| = 1$ . Consequently, some tradeoff is necessary for completing the design. It is suggested here to use the control effort weighting function  $W_{un}(s)$  as a tuning parameter in the design process, explanation follows.

After  $W_s(s)$  is calculated we proceed to obtain the optimal compensator  $G(s)$  by one of the known algorithms that solve the  $H_\infty$ - norm optimization. In this first design stage, use a low gain  $|W_{un}(j\omega)|$ . This is equivalent to accepting large effort signals due to command and disturbance inputs, and if the sensor noise is concerned, high sensor noise amplification  $T_{un} = u/n$  is then expected. With this assumption, the  $H_\infty$  control solution will tend to have very high gains open-loop TFs, consequently, also low gain sensitivity functions, and overdesign is achieved despite of the correctly defined nominal sensitivity function  $|S_n(j\omega)|$ . With this initial solution, draw the Bode plots of  $|T_1(j\omega)|$  for  $\forall \{P\}$  and check if the changes are smaller than as permitted by the specified upper and lower tracking bounds. If so, augment  $|W_{un}(j\omega)|$  which will lead to an  $H_\infty$  control solution with lower open-loop gains, or higher sensitivity function gains, in other words, with reduced sensitivity characteristics for the input/output TF  $T_1(s)$ .

Check again the maximum gain changes in  $|T_1(j\omega)|$  and repeat this process until the maximal changes comply with the permitted bounds.

This completes the first stage of the design in which the compensator  $G(s)$  is derived. In the second stage, the prefilter  $F(s)$  is designed so that all  $|T_1(j\omega)|$ s are driven inside the permitted bounds on  $|T(j\omega)| = |F(j\omega)T_1(j\omega)|$ , as in the *QFT* solution. Generally, no more than two to three iterations with different  $|W_{un}(j\omega)|$  are necessary, as will be demonstrated in Example 1. The different steps of the design process using the  $H_\infty$ -norm optimization for solving the uncertain plant TDOF problem with multiplicative perturbation modeling are summarized as follows.

- Step 1.** Translation of the time domain specifications to frequency domain specifications.
- Step 2.** Choice of a nominal plant and the plant weighting function  $W_{MP}(s)$  for robust stability.
- Step 3.** Calculation of the sensitivity weighting function  $W_s(s)$ , based on Eq.(23), and a first try low gain  $W_{un}(s)$  weighting function.
- Step 4.** Solve the norm optimization, Eq.(14), use for instance *hinfsyn* in the  $\mu$ -Analysis and Synthesis Toolbox or *hinflmi*, *hinfric* in the LMI Toolbox.
- Step 5.** Use the obtained semi-optimal controller  $G(s)$  to calculate  $|T_1(j\omega)|$  for extreme plant cases. If the maximal changes in  $|T_1(j\omega)|$  are exactly satisfied by the specified upper and lower bounds of  $|T(j\omega)|$  at some frequencies, then proceed to Step 6. If not, repeat Step 5 with a modified  $W_{un}(s)$  weighting function until the maximal changes in  $|T_1(j\omega)|$  exactly satisfy the maximal permitted changes at some frequencies. Then proceed with Step 6.
- Step 6:** Design the prefilter  $F(s)$  as to locate all  $|T_1(j\omega)|$ s inside the permitted bounds.  
 $|T(j\omega)| = |F(j\omega)| |T_1(j\omega)|$
- Step 7.** Evaluation of the design in the time and frequency domains and refinement of the solution if necessary.

The following example illustrates the above design procedure.

**Example 1.**  $P(s) = k/(s+\alpha)(s+b)$ ;  $k = [1-10]$ ,  $\alpha = [1-5]$ ,  $b = [0.2-1]$ . The tracking input/output specifications in the frequency domain must lie between the upper and lower bounds shown in Figs.(5),(6)and (7). Maximum allowed peaking in  $S$  and  $T_1$  are:  $\beta = |T_1(j\omega)|_{\max} = 3db$ ;  $\gamma = |S(j\omega)|_{\max} = 3db$ . Use  $H_\infty$  design technique to achieve a solution satisfying the above specification under the constraint of minimizing as much as possible the sensor noise amplification.

**Solution:** The solution of this problem follows the above design stages.

**Step 1.** The permitted changes in  $|T(j\omega)|$ db are shown in Fig.5, from which  $\Delta|T(j\omega)|$  are extracted.

**Step 2.** In practice,  $\left| \frac{P(j\omega)}{P_n(j\omega)} - 1 \right|$  is plotted for different choice of  $P_n(s)$  until the most favorable one is detected in the sense that the lowest gain  $|W_{MP}(j\omega)|$  is attained. In this example  $P_n(s) = 10/(s+0.2)(s+1)$  was the most favorable choice, attaining a maximum value of 0.95 for  $|P/P_n - 1|$ . Hence, let us choose  $W_{MP}(s) = 0.95$ .

**Step 3.** The choice of  $W_s(s)$  is more complicated. To find the nominal specifications of  $S(s)$ ,  $|P(j\omega)/P_n(j\omega)|$  for most of the plant cases can be calculated and the maximum  $\Delta|P(j\omega)|_{\max}$  for the chosen frequencies used in the table below. Since  $\Delta|T(j\omega)|_{\max}$  is known from the permitted bounds shown in Fig.5, Eq.(23) can be used to calculate the needed  $|S(j\omega)|$ , see Table 1.

**Table 1.** Data for calculating  $W_s(s)$  that satisfy the sensitivity bounds in Figs.5,6 and 7.

$\omega$ rad/sec	0.2	0.3	0.5	0.7	1	1.5	2	3
$\Delta T _{\max}$ dB	0.4	1	2	4	6	11	13	17
$\Delta P _{\max}$ dB	42	38	36	34	34	30	28	25
$ S _{\text{db}}$	-40	-32	-25	-19	-15	-9	-7	-3

A little cut and try on the Bode diagram allows to find a  $1/W_s(s)$  that slightly oversatisfies  $|S(j\omega)|$  in the table in order to be on the safe side for the first trial design

$$W_s(s) = \frac{(s+5)(s+7)}{1.5(s+0.01)(s+0.1)}. \quad W_{un}(s) \text{ is chosen initially as } W_{un}(s) = 0.001$$

**Step 4-1.** The compensator  $G(s)$  is obtained by solving the  $H_\infty$  norm sensitivity problem with the aid of *hinfsyn* algorithm in  $\mu$ -Analysis and Synthesis Toolbox. The detailed program for the solution is not shown for lack of space.  $G(s)$  is found to be

$$G(s) = 1.66 \times 10^9 \frac{(s+0.1997)(s+1)(s+1.695)}{(s+0.01)(s+0.1)(s+164.41)(s+2.146 \times 10^6)}$$

**Step 5-1.** The obtained semi-optimal controller  $G(s)$  is used to calculate  $|T_1(j\omega)|$  for all plant cases. These are shown in Fig.5. It is not surprising that all resulting  $|T_1(j\omega)|$ s lie outside the permitted upper and lower bounds, also shown. However, it is also observed that the overall changes in  $|T_1(j\omega)|$  are much smaller than allowed by the permitted bounds at all frequencies, in other words, an overdesign was achieved with too high open-loop gains which cause unnecessarily increased sensor noise amplification. Return to Step 4 for ameliorating the solution with a second choice of  $W_{un}(s)$ .

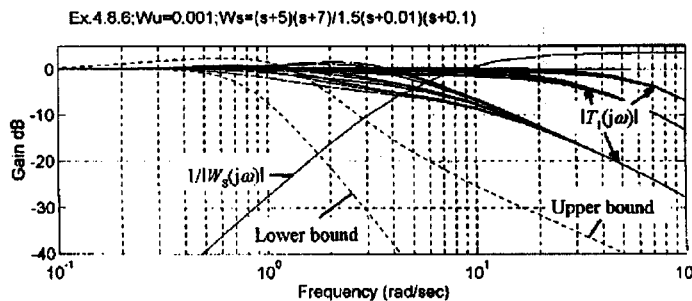


**Figure 5.**  $|T_1(j\omega)|$ s Bode plots, 1st trial design.

**Step 4-2.** For the second design trial  $W_{un}(s)$  is readjusted to  $W_{un}(s) = 0.007$ . After rerunning the  $H_\infty$  design program the following compensator is derived

$$G(s) = 1.906 \times 10^8 \frac{(s + 0.2)(s + 1)(s + 2.02)}{(s + 0.01)(s + 0.1)(s + 63.59)(s + 1.46 \times 10^6)}$$

**Step 5-2.** The obtained semi-optimal controller  $G(s)$  is once again used to calculate  $|T_1(j\omega)|$ s for all plant cases. These are shown in Fig.6. It is observed that the changes in the gains of  $|T_1(j\omega)|$  at the frequency range  $\omega = 0.4$  to  $0.7$  r/s match exactly the permitted bounds and are lesser than these bounds for higher frequencies.

**Step 6:** A simple prefilter  $F(s)$  is used to achieve the tracking closed loop specifications. It is designed so as to relocate all  $|T_1(j\omega)|$ s inside the permitted bounds on  $|T(j\omega)|$ , see Fig.7. With the prefilter

$$F(s) = \frac{2.727(s + 0.22)}{(s + 0.3)(s + 1)(s + 2)}$$

the second degree of freedom specifications are completely achieved.

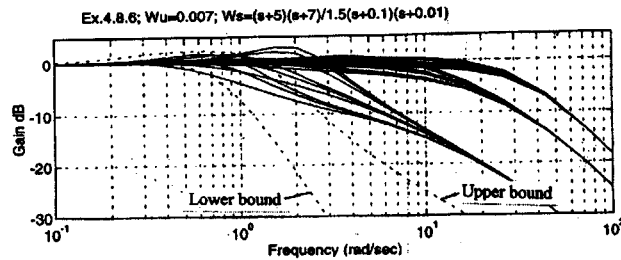


**Fig.6 .**  $|T_1(j\omega)|$ s Bode plots, 2nd trial design.

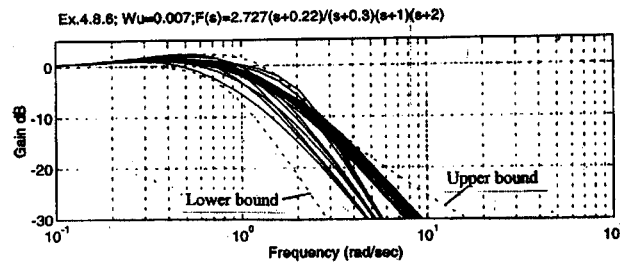


**Figure 7 .**  $|T(j\omega)| = |F(j\omega)| |T_1(j\omega)|$  Bode plots.

It is of interest for comparison purposes to show the achieved nominal sensitivity function  $|S_n(j\omega)|$  versus  $1/|W_s(j\omega)|$ , see Fig.8 on which are also shown  $|T_{1n}(j\omega)|$  and  $|T_n(j\omega)|$ . The obtained nominal  $|S_n(j\omega)|$  does not follow exactly the specified  $1/|W_s(j\omega)|$ , but this is a direct

consequence of the inability of the optimizing  $H_\infty$  -norm design technique to satisfy exactly both  $|S_n(j\omega)|$  and  $|T_{1n}(j\omega)|$ , remember that  $S(s) + T_1(s) = 1$  !

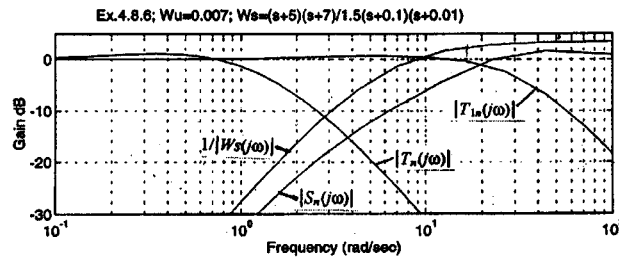


**Figure 8.**  $1/W_s(j\omega)$  ,  $|T_{1n}(j\omega)|$  ,  $|T_n(j\omega)|$  and  $|S_n(j\omega)|$  Bode plots.

**Step 7.** Evaluation of the design follow.

**1- Stability margins.** The open-loop TFs on Nichols chart (NC) for all the set  $\{P\}$  are shown in Fig.9. It is important to realize that none of the open-loop TFs exceeds the contours of  $|T_1| = 3\text{db}$  and  $|S| = 3\text{db}$  as required, so that no large overshoots in the time domain will occur for disturbances. Moreover, for the same reason, large gain and phase margins are achieved, at least 17 db and  $50^\circ$  respectively.

**2- Step time response.** As can be seen from Fig.10, the step time responses for all the family of plants are well inside the permitted bounds.

**3- Sensor noise amplification.** Sensor noise amplification is one of the most difficult problems in control engineering. Large noise amplification can preclude the possibility of using preferred engineering practical control schemes, Sidi (1997).

The control compensator achieved in Step 4-2 shows that in practice it is a TF with the same number of poles and zeros (one of the poles is located at  $s = -1.46 \cdot 10^6$ ) hence a tremendous noise amplification  $u/n = T_{un}$ , (Fig .4a), is to be expected, leading to a control effort that cannot be maintained. This RMS amplification was computed for all plant cases and the results was an average amplification of  $1.1147 \cdot 10^5$  (RMS) ! Practically, with such a tremendous noise amplification, no engineering solution exists.

A noise filter is to be added to the nominally obtained  $G(s)$  with the  $H_\infty$  control optimization algorithm using classical frequency design methods. When a filter  $100/(s+100)$  is added, the average noise amplification decreased to 746 (RMS) which is acceptable from engineering point of view. The results in Figs.6, 7, 9 and 10 are obtained with the modified compensator including the noise filter. For comparison purposes, if the same problem is solved with the  $QFT$  design procedure, (using the  $QFT$  Toolbox), the average noise amplification is about 1000 (RMS), which is practically the same result achieved with the  $H_\infty$  design procedure. The time response of both designs are also very similar.

This completes the design of Example 1.

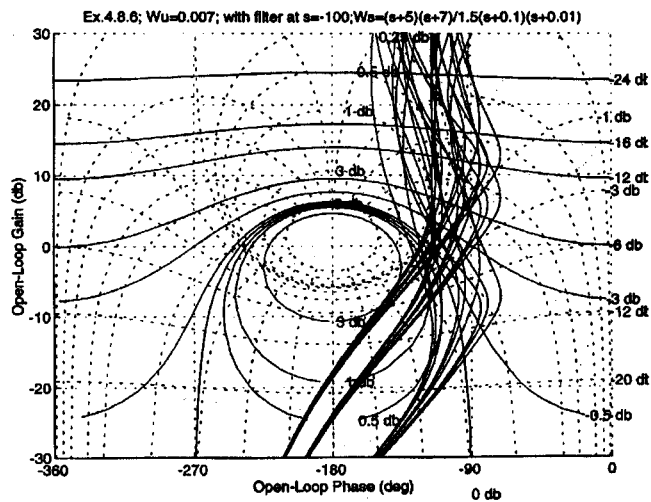


**Figure 9.** Nichols diagram plots of open-loop TFs. Solid lines contours:  $|S|$  in inverted NC. Dashed line contours:  $|L/(1+L)|$  in the NC.

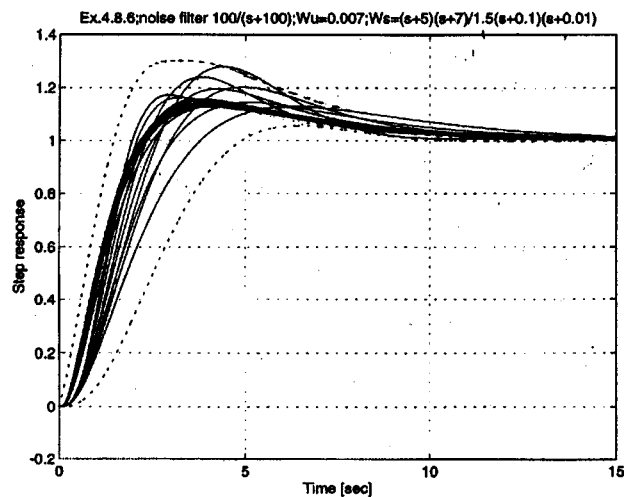


**Figure 10.** Step time responses for some extreme plant cases.

#### 4. The MIMO case.

The design procedure for the TDOF MIMO problem using the  $H_\infty$  design technique follows almost exactly the same procedure explained in the previous section. The difference is in the use of 'principal gains' for characterizing magnitudes when matrices are dealt with, instead of using the classical 'gains' for algebraic feedback systems. For lack of space, the MIMO TDOF case for uncertain feedback systems will not be treated in length. Basic lines of the solution will be only cited.

Similarly to the SISO case, tracking closed-loop input/output specifications for each of the  $n$  channels are defined in upper and lower permitted bounds; in a  $n \times n$  MIMO feedback system, a  $n \times n$  transfer matrix including  $n^2$  tracking transfer functions is specified. All weighting functions become weighting transfer matrices, with each element pertaining to the equivalent physical channel. The only major difference is the way in which the uncertainty of the MIMO plant is represented, so that robust stability can be guaranteed. Based on the definition of matrix uncertainty, conditions for robust stability can be also stated.

#### 4.1 Uncertainty modeling of MIMO plants.

There exist multiple ways of modeling uncertainties of MIMO systems, a common one being once more the *multiplicative perturbation modeling*. As for the SISO case, different kinds of uncertainties can be lumped in this model. However, in the MIMO case the uncertainty can be defined at the input, or the output of the MIMO plant, depending on where the loop is opened.

##### 1- Output uncertainty

$$\mathbf{P}(s) = [\mathbf{I} + w_o(s)\Delta_o(s)]\mathbf{P}_n(s) \quad \|\Delta_o\|_\infty \leq 1 \quad (24)$$

where  $w_o(s)$  is a scalar weight, see Skogestad and Postletwaite (1996).

Exactly as for the SISO case we can find a limiting frequency dependent function satisfying the maximum principal gains of the matrix plant perturbations

$$\delta_o(\omega) = \max_{\mathbf{P} \in \{\mathbf{P}\}} \bar{\sigma}[(\mathbf{P} - \mathbf{P}_n)\mathbf{P}_n^{-1}(j\omega)] \quad (25)$$

and

$$|w_o(j\omega)| \geq \delta_o(\omega) \quad \forall \omega$$

##### 2- Input uncertainty

In a similar way, for the multiplicative input perturbation,

$$\delta_i(\omega) = \max_{\mathbf{P} \in \{\mathbf{P}\}} \bar{\sigma}[\mathbf{P}_n^{-1}(\mathbf{P} - \mathbf{P}_n)(j\omega)] \quad (26)$$

and

$$|w_i(j\omega)| \geq \delta_i(\omega) \quad \forall \omega$$

With this definition and limiting weighting functions based on the maximum principal gains of the matrix perturbations, an important theorem on MIMO robust stability has been proven by different authors, Doyle and Stein (1981), Lehtomaki (1981), Stein and Athans (1987), and others. This theorem is very similar to that pertaining to the SISO case and states that when the perturbation is defined as in Eq.(24), robust stability is maintained if and only if the nominal unity feedback tracking matrix

$$\mathbf{T}_{ufn}(s) = \mathbf{P}_n(s)\mathbf{G}(s)[\mathbf{I} + \mathbf{P}_n(s)\mathbf{G}(s)]^{-1} \quad (27)$$

satisfies the inequality

$$\bar{\sigma}[\mathbf{T}_{ufn}(j\omega)] \leq \frac{1}{w(\omega)} \tag{28}$$

The subscript (<sub>n</sub>) in the above equations stand for the nominal plant case.

**4.2. Design procedure for the MIMO uncertain case.**

With the definitions and the robust stability theorem in the last section, design procedure for the TDOF MIMO case follows exactly the procedure for the SISO case with the difference that we deal now with matrices. A 2x2 system design example follows.

**Example 2.** There is given an uncertain plant MIMO system  $p_{ij}(s) = k_{ij}(1+s/A_{ij})$  with plant uncertainties defined in Table 3 below for nine plant cases .

**Table 3. MIMO plant parameters**

Case No	$k_{11}$	$k_{22}$	$k_{12}$	$k_{21}$	$A_{11}$	$A_{22}$	$A_{12}$	$A_{21}$
1	1	2	0.5	1	1	2	2	3
2	1	2	0.5	1	0.5	1	1	2
3	1	2	0.5	1	0.2	0.4	0.5	1
4	4	5	1	2	1	2	2	3
5	4	5	1	2	0.5	1	1	2
6	4	5	1	2	0.2	0.4	0.5	1
7	10	8	2	4	1	2	2	3
8	10	8	2	4	0.5	1	1	2
9	10	8	2	4	0.2	0.4	0.5	1

**Solution:**

**Step 1.** The specified bound on the transfer function  $|T_{11}(j\omega)|$  and  $|T_{22}(j\omega)|$  are shown in Figs.13 and 14 together with the achieved closed-loop TFs. From these bounds, permitted changes  $\Delta|T_{ij}(j\omega)|$  are extracted for the next design steps. Design specifications ask for minimizing the transfer between channels,  $|T_{12}(j\omega)|$  and  $|T_{21}(j\omega)|$ , so that initially they are put to zero.

**Step 2.** To find the limiting weighting matrix for the plant perturbations, Eq.(26) or (28) are calculated with different nominal plant conditions until the lower  $\delta(\omega)$  is obtained. In this example case 9 was chosen as the nominal case,  $\delta(\omega)$  was calculated for the remaining plant cases, the results are shown in Fig. 11. It is easily found that a limiting multiplicative perturbation weighting function is  $w_o(\omega) \equiv w_{MPo}(\omega) = 0.92(s+1)/(s/1.09+1)$  which is also shown in the same figure.

**Step 3.** Permitted changes of  $\Delta|T_{ij}(j\omega)|$  are specified in Fig. 13, see also Table 4. In the MIMO problem,  $\Delta\sigma(\mathbf{P}(j\omega))_{\max}$  is used in calculating the sensitivity function  $S_{11}(s)$  and  $S_{22}(s)$  because the maximum changes in principal gains (Fig. 12) are larger than the gain changes of all individual elements of the transfer matrix  $\mathbf{P}$ , see Table 4. In this way, the uncertainties in  $P_{12}$  and  $P_{21}$  are also taken into consideration when designing the  $T_{11}$  and  $T_{22}$  channels. From this data  $w_{S11}(s)$  and  $w_{S22}(s)$  are approximated as

$$w_{S11}(s) = 0.7(s+12)/(s+0.01) \text{ and}$$

$$w_{S22}(s) = 0.7(s+80)(s+0.01).$$

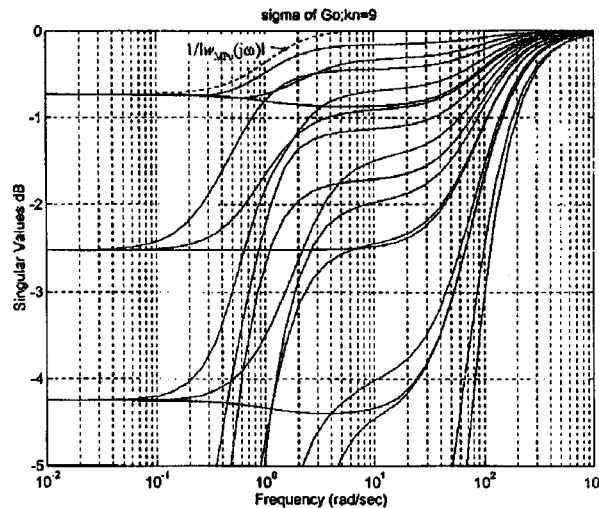


**Figure 11.** Principal gains of  $\sigma[(\mathbf{P} - \mathbf{P}_n)\mathbf{P}_n^{-1}(j\omega)] \quad \forall \{P\}$  for evaluating  $w_{MP0}(\omega)$ .

**Table 4.** Data for calculating the needed sensitivity functions  $S_{11}$  and  $S_{22}$ .

$\omega$ rad/sec	0.2	0.5	1	2	5	10	20
$\Delta\sigma_{\max}\mathbf{P}$	27	26	26	30	31	33	35
$\Delta T_{11}$ (db)	1	2.5	7	12	22	30	-
$\Delta P_{11}$ (db)	20	20	22	26	33	35	37
$S_{11}$ (db)	-28	-20	-12	-8	-3	-1	-
$\Delta T_{22}$ (db)	0.1	0.2	1	3.5	9	13	15
$\Delta P_{22}$ (db)	12	15	19	23	26	28	28
$S_{22}$ (db)	-47	-42	-28	-19	-11	-8	-8

**Step 4-1.** The compensator  $G(s)$  is obtained by solving the  $H_\infty$  norm sensitivity problem with the aid of *hinfsyn* algorithm in  $\mu$ -Analysis and Synthesis Toolbox. In a first trial design, choice for the control effort weighting functions matrix  $\mathbf{W}_u(s)$  was as follows:

$$w_{u11} = 0.5; w_{u22} = 1; \mathbf{W}_u(s) = \text{diag}(0.5, 1)$$

**Step 5-1.** With the choice in Step 4-1, the sensitivity specifications for  $|T_{11}(j\omega)|$  were completely satisfied.

However, the changes in  $|T_{22}(j\omega)|$  at low frequencies were larger than allowed by the design specifications.

**Step 4-2.**  $W_u(s)$  was readjusted as follows:

$w_{u11} = 0.5$ ;  $w_{u22} = 0.5$  so that the  $T_{22}$  channel is affected adequately, finally,  $W_u(s) = \text{diag}(0.5, 0.5)$  and the design was repeated using the *hinfsyn* algorithm. The elements of the compensating matrix  $G(s)$  are after cancellation of very close poles and zeros

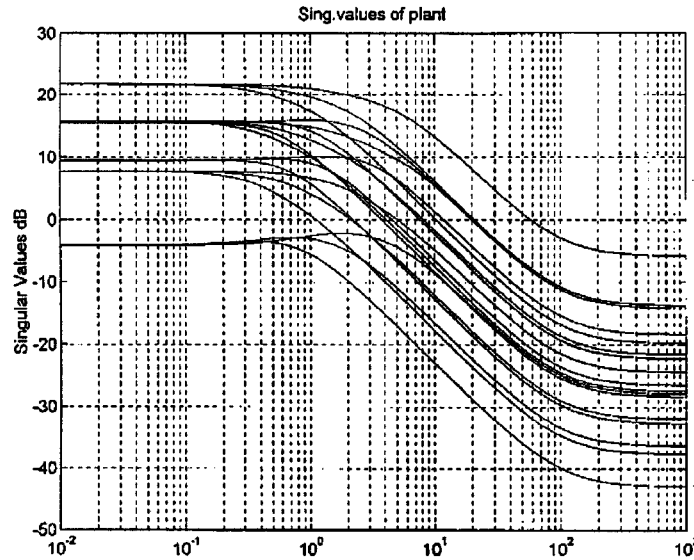


**Figure 12.** Principal gains of  $P(j\omega)$  for all plant conditions.

$$G_{11}(s) \cong 6.77 \frac{(s+5)(s+1.09)(s+0.9997)}{(s+142.4)(s+1.1383)(s+0.904)(s+0.01)}$$

$$G_{22}(s) \cong 1.973 \times 10^5 \frac{(s+2.5)(s+1.09)(s+0.983)}{(s+4417)(s+1.155)(s+0.904)(s+0.01)}$$

$$G_{21} \cong -518.8 \frac{(s+151)(s+4.995)(s+2.5)(s+1.09)}{(s+4417)(s+142.48)(s+1.138)(s+0.904)(s+0.01)}$$

$$G_{12}(s) \cong 266.989 \frac{(s-588.7)(s+5)(s+2.64)(s+1.09)(s+1)}{(s+4417)(s+142.48)(s+2.022)(s+1.155)(s+0.904)(s+0.01)}$$

**Step 5-2.** The obtained semi-optimal controller  $G(s)$  was once more used to calculate the unity feedback  $|T_{uf11}(j\omega)|$  and  $|T_{uf22}(j\omega)|$ . They are shown in Fig.(13) *a* and *b* respectively. The changes in the unity feedback TFs gains satisfy completely the sensitivity specifications.

**Step 6-2.** Prefilters  $F_{11}(s)$  and  $F_{22}(s)$  are designed for both channels in order to relocate the unity feedback transfer functions  $|T_{uf11}(j\omega)|$  and  $|T_{uf22}(j\omega)|$  inside the permitted bounds of  $|T_{11}(j\omega)|$  and  $|T_{22}(j\omega)|$ ;

$$F_{11}(s) = 0.6(s+3.25)(s+1/3.25)/(s+1)^2(s+0.6); \quad F_{22}(s) = 90/(s+3)(s+30)$$

The final resulting transfer functions  $|T_{11}(j\omega)| = |F_{11}(j\omega) T_{uf11}(j\omega)|$  and  $|T_{22}(j\omega)| = |F_{22}(j\omega) T_{uf22}(j\omega)|$  for all plant conditions are shown in Fig.14 *a* and *b*. The design specifications for tracking are completely achieved. In Fig.15 are shown the cross-channel TFs. They cannot stay null as wished because of plant uncertainties, but they are practically very low as expected. The defined weighting functions  $1/w_{s11}$  and  $1/w_{s22}$  and the achieved  $|S_{n11}(j\omega)|$  and  $|S_{n22}(j\omega)|$  are shown in Fig.16. On the same figure are also shown the achieved nominal  $|T_{uf11}(j\omega)|$  and  $|T_{uf22}(j\omega)|$ .

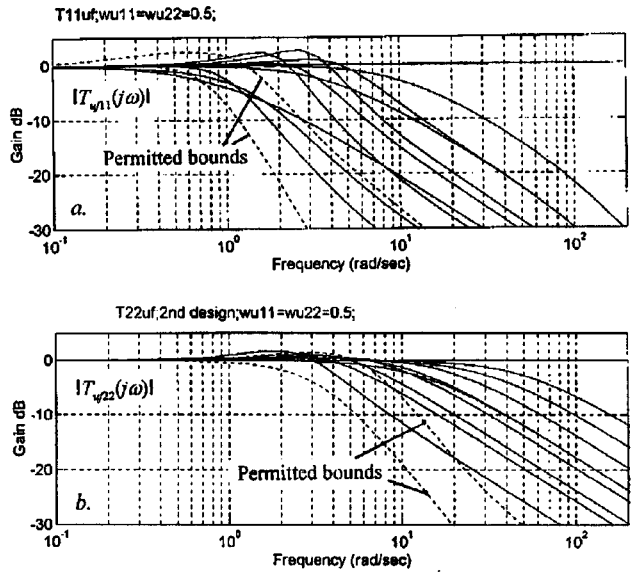


Figure 13.  $|T_{uf11}(j\omega)|$  and  $|T_{uf22}(j\omega)|$  ODEF unity feedback solution, no prefilters.

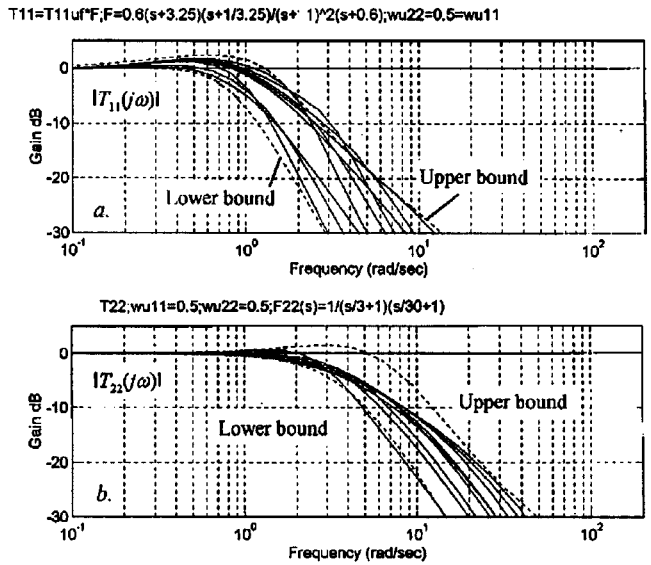


Figure 14.  $|T_{11}(j\omega)|$  and  $|T_{22}(j\omega)|$  TDOF solution with prefilters  $F_{11}(s)$  and  $F_{22}(s)$

**Step 7.** Evaluation of the design follow.

**1- Stability margins.** The open-loop TFs on Nichols chart are shown for both channels in Figs.17 and 18. Exactly as in the SISO Example 1, it is important to realize that none of the open-loop TFs exceeds the contours of  $|T_1| = 3\text{db}$  and  $|S| = 3\text{db}$  as required, so that no large overshoots in the time domain will occur for disturbances. Moreover, for the same reason, large gain and phase margins are achieved, at least 17 db and  $50^\circ$  respectively.

**2- Step time response.** As can be seen from Fig.19, the step time responses for all the family of plants are well inside the permitted bounds. Interchannel responses are also shown, their amplitudes are negligible.

**3- Disturbance responses.** It is of importance to check the attenuation of disturbances, whose frequency responses are shown in Fig.20.

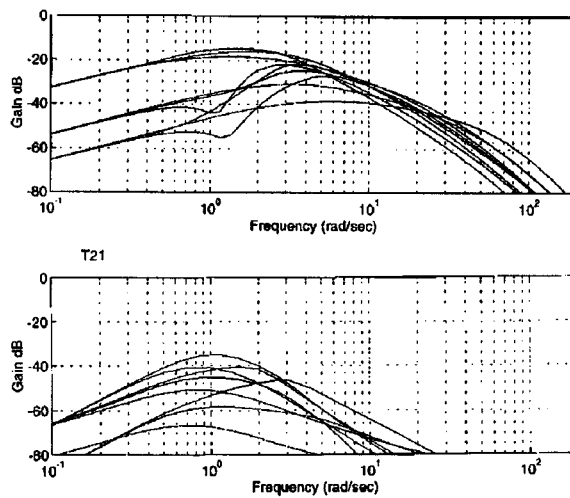


**Figure 15.**  $|T_{12}(j\omega)|$  and  $|T_{21}(j\omega)|$ .

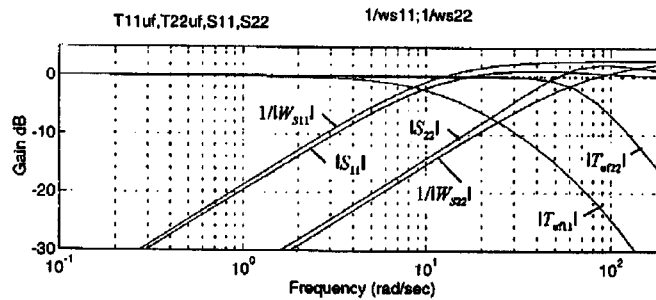


**Figure 16.** Achieved  $|T_{11}(j\omega)|$ ,  $|T_{22}(j\omega)|$ ,  $|S_{n11}(j\omega)|$ ,  $|S_{n22}(j\omega)|$ , and the specified  $1/w_{s11}$ ,  $1/w_{s22}$ .

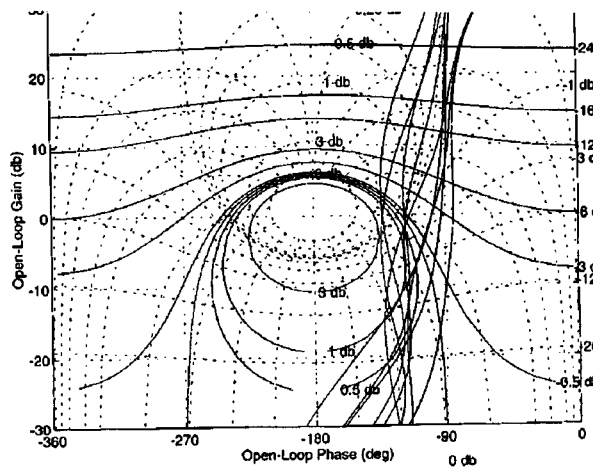


Figure 17. Open-loop TFs  $L_1(j\omega)$  opened at  $u_1$  for all plant conditions

**4- Sensor noise amplification.** The control compensator achieved in Step 4-2 shows that in practice it is a TF with the same number of poles and zeros (one of the poles of all  $G_{ij}(s)$  are located very far from the active frequency range) hence a high noise amplification of the sensor noise generators to the control signals  $u_1$  and  $u_2$  can exist (Fig .4) leading to a control effort that cannot be maintained. A noise filter is to be added to

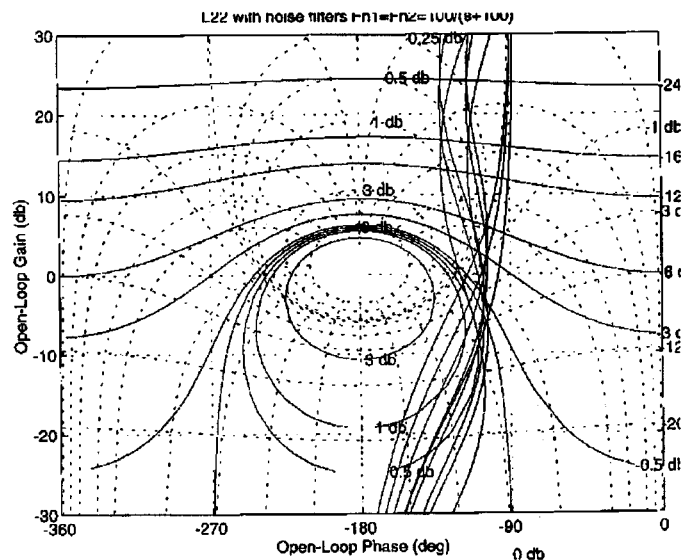
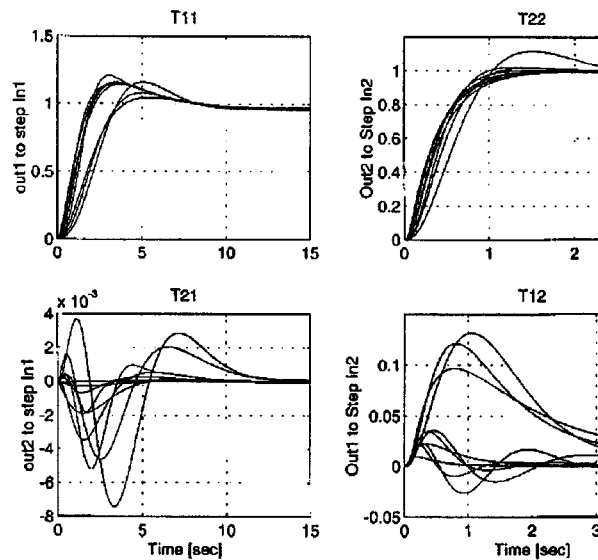
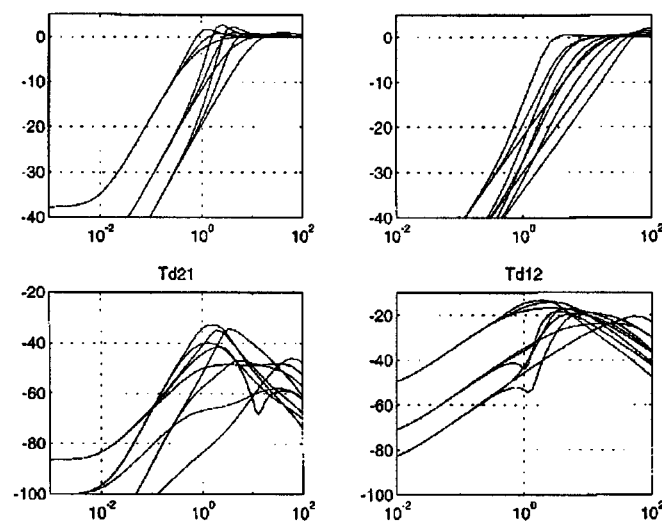


Figure 18. Open-loop TFs  $L_2(j\omega)$  opened at  $u_2$  for all plant conditions



**Figure 19.** Step time responses at  $In_1$  and  $In_2$  for all plant conditions



**Figure 20.** Frequency Responses to disturbances

the nominally obtained  $G(s)$  with the  $H_\infty$  control optimization algorithm using classical frequency design methods. When a filter  $100/(s+100)$  is added, the average noise amplification for both channels is quite low, in the order of 1.2 (RMS) for the first and 18.3 (RMS) for the second channel which is acceptable from engineering point of view. The results in Figs.13 to 20 are obtained with the modified compensator including the noise filter.

## 5. Summary and conclusions.

Using the proposed TDOF  $H_\infty$  - design technique for uncertain plants, it is seen that the specifications are completely achieved, with two to three design iterations at most. Specified tracking characteristics in the time domain are achieved by translating them as upper and lower permitted bounds in the frequency domain, exactly as in the QFT design technique. Acceptable noise amplification is achieved by manipulating the nominal open-loop TF in the higher frequency range with classical Nyquist/Bode frequency design techniques. The technique works adequately for both SISO and MIMO uncertain systems.

## References

- Doyle J., (1978), "Robustness of Multiloop Linear Feedback Systems", Proc. 17th IEEE Conference Decision and Control, pp.12-18.
- Doyle J., and Stein G., (1981), "Multivariable Design: Concepts for a Classical/Modern Synthesis", IEEE Trans. on Automatic Control, vol. AC-26, no.1, February.
- Doyle J., (1983), "Synthesis of robust controllers and filters ", Proc.IEEE Conf. on Decision and Control, San Antonio, Texas, pp.109-114.
- Doyle J., (1986), "Quantitative Feedback Theory (QFT) and Robust Control", Am. Control Conf.,1986, pp.1691-1698.
- Yaniv O. and Horowitz I., (1987) "Quantitative feedback theory -reply to criticism", Int.J.Control, 46(3), 945-962.
- Francis B. and Doyle J., (1986), "Linear control theory with an optimality criterion", SIAM J. Control Opt.
- Doyle J., Francis B. and Tannenbaum A., (1992), *Feedback Control Theory*, Macmillan Publishing Company.
- Horowitz I.,(1963), *Synthesis of Feedback Systems*, Academic Press, New York, London
- Horowitz I. and Sidi M., (1972), "Synthesis of feedback systems for prescribed time-domain tolerances", INT.J. CONTROL, vol.16, No. 2, 287-309.
- Horowitz I.,Sidi M., (1978):"Optimum synthesis of non-minimum phase feedback systems with plant uncertainty, INT.J.CONTROL, vol. 27, No.3, 361-386
- Kwakernaak H., (1993), "Robust Control and H-Optimization-Tutorial Paper", Automatica, 29(2), pp.255-273.
- Lehtomaki N., (1981), "Practical robustness measures in multivariable control", Ph.D. dissertation, Mass. Inst.Techol., Cambridge, MA, May.
- Sidi M.,(1976), "Feedback Synthesis with Plant Ignorance, Nonminimum-Phase, and Time-Domain Tolerances", Automatica, Vol. 12, pp 265-271.
- Sidi M.,(1977), : "Synthesis of sampled feedback systems for prescribed time domain tolerances, vol. 26, No.3, 445-461.
- Sidi M., (1997), *Dynamics and Control of Spacecraft-practical engineering approach*, Cambridge University Press.
- Skogestad S. and Postletwaite I., (1996), *Multivariable Feedback Control*, John Wiley & Sons, Chichester, New York,
- Stein G. and Athans M., (1987), "The LQG/LQR Procedure for Multivariable Feedback Control Design", IEEE Trans. on Automatic Control, vol. AC-32, no.2, February.

- Zames G.,(1976)," Feedback and copmplexity", IEEE Conf. Dec. Control
- Zames G., (1981), "Feedback and optimal sensitivity: model reference transformations, multiplicative seminorms, and approximate inverses", IEEE Trans. Auto.Contr., vol.AC-26, pp.301-320.
- Zames G. and Francis B.,(1983)," Feedback, minimax sensitivity, and optimal robustness", IEEE Trans. Auto. Contr., vol.AC-28, pp.585-601..
- Zhou K. and Doyle J.,(1998), *Essentials of Robust Control*, Prentice Hall, New Jersey